Electrocatalyzed Direct Arene Alkenylations without Directing Groups: Selective Late-Stage Drug Diversification

Lutz Ackermann (✉ Lutz.Ackermann@chemie.uni-goettingen.de)
Georg-August-University Göttingen https://orcid.org/0000-0001-7034-8772
Zhipeng Lin
Georg-August-University Göttingen
Uttam Dhawa
Georg-August-University Göttingen
Binbin Yuan
Georg-August-University Göttingen
Yan-Cheng Liou
Georg-August-University Göttingen
Magnus Johansson
AstraZeneca Gothenburg https://orcid.org/0000-0002-0904-2835

Physical Sciences - Article

Keywords:

Posted Date: May 5th, 2022

DOI: https://doi.org/10.21203/rs.3.rs-1607467/v1

Version of Record: A version of this preprint was published at Nature Communications on July 15th, 2023. See the published version at https://doi.org/10.1038/s41467-023-39747-0.

Abstract

Electrocatalysis has emerged as an increasingly viable platform for molecular syntheses, that can replace chemical redox agents and enable unprecedented reaction pathways. Despite major progress in electrooxidative C–H activations, these arene transformations generally require directing groups for chelation-induced efficiency and control of position-selectivity in the C–H activation. The installation and removal of these directing groups calls for additional synthesis operations, which jeopardizes the inherent efficacy of the C–H activation approach in terms of undesired waste formation and low resource economy. In sharp contrast, we herein present molecular electrocatalyzed C–H olefinations of simple arenes devoid of exogenous directing groups. The robust palladaelectro-catalysis proved amenable to a wide range of both electronically-diverse arenes under exceedingly mild reaction conditions. The strategy avoids sacrificial chemical oxidants, but operates by the reductive hydrogen evolution reaction (HER). This study points to a remarkable strategy comprising two electrochemical transformations to guarantee unprecedented levels of position-selectivities in direct arene olefinations. Cyclic voltammetry studies and computational analysis identified a direct correlation between the redox potential and catalysis efficacy. The palladaelectro-catalysis strategy avoids protecting and directing group interconversions, the practical importance of which is reflected by direct late-stage functionalizations of structurally complex compounds of relevance to drug discovery and pharmaceutical industries.

Main Text

In recent years, molecular electro-organic synthesis has surfaced as uniquely effective toolbox for sustainable organic syntheses.[1-6] Despite indisputable progress through merging electrosynthesis and metal catalysis,[7-11] electrochemical C–H activations continue to be severely restricted to directing groups (DG), which guarantee chelation-induced efficiency and selectivity in intermolecular C–H activations.[12-21] The installation and removal of the DGs require additional synthesis and purification operations, leading to undesired waste formation and low overall resource-efficiency (**Fig. 1a**). While major advances have been noted in selective[22-25] catalyst-guided C–H activations,[26-46] they are severely limited by the need for super-stoichiometric amounts of often toxic or cost-intensive terminal chemical oxidants, typically representing a major obstacle on scale (**Fig. 1b**). In contrast, we have devised DG-free C–H olefinations under exceedingly mild reaction conditions by means of molecular electrocatalysis (**Fig. 1c**). This strategy combines a synthetically useful molecular transformation with the HER for a decentralized green hydrogen economy, and is characterized by outstanding position-selectivities through the judicious choice of the electrode material to enable a twofold electrooxidation (**Fig. 1d**). The potential of the DG-free approach was mirrored by the late-stage electro-diversfication of structurally-complex molecules of relevance to drug discovery and chemical biology (**Fig. 1e**).

We initiated our studies towards the DG-free electrochemical C–H activation by evaluating several ligands,[27-28] (**Fig. 2a** and **Supplementary Table S5**). We thus observed considerable electrocatalytic activity with pyridine **L1** in the absence of DGs with electricity as the redox agent. Variation of the

pyridone ligand motif resulted in an increased efficacy, while amino acid derivatives **L5-L6** and 4,5-diazafluoren-9-one (**L7**) afforded inferior results. It is noteworthy that improved performance was observed with *S*-ligands **L8-L12**,[40-42,46] leading to almost quantitative conversion to the olefination product **3** with *S,O*-ligand **L12**.

To rationalize the observed catalysis performance, we explored a direct correlation with the catalyst oxidation behavior.[47] Hence, the onset oxidation potential for the *in-situ* generated palladium catalyst in the presence of the *S,O*-ligand **L12** was observed at 1.35 V_{SCE}, thus 200 mV lower than the one of the complex derived from N-ligand **L2**, directly correlating the inherently higher reactivity (**Fig. 2b**). The low catalytic efficiency of the bipyridine-based palladium complex was likewise correlated with an oxidation potential of 1.70 V_{SCE}. Further optimization revealed a detrimental effect of *n*-Bu_4NOAc as supporting electrolyte or TFE and AcOH as a solvent mixture (**Fig. 2c**, entries 2-4). The beneficial effect of benzoquinone (BQ) is suggestive of a redox mediator role and a prevention of palladium(0) aggregation (entry 5). Control experiments revealed the necessity of the palladium catalyst, the ligand and the electricity for the DG-free electrochemical C–H activation (entry 6-8).

With the optimized electrolysis conditions in hand, we probed the robustness of the DG-free electrocatalyzed olefination (**Fig. 2d**). We found that both electron-rich and challenging electron-poor arenes **1** delivered the mono-olefinated products in good to excellent yields by the palladium-electrocatalysis. Thus, arenes **1b** and **1c** provided the styrene derivatives **4** and **5**, respectively. A wide range of monosubstituted arenes **1d**-**1g** was selectively functionalized, including unprotected *OH*-free phenol **1g** (**9**). When using disubstituted arene substrates, the position-selectivity was largely governed by repulsive steric interactions. Tetrahydronaphthalene (**1h**) afforded predominantly the *b*-isomer **10**. Dimethoxybenzene (**1i**) exclusively yielded the *b*-olefinated product **11**, while 1,3-disubstituted arenes **1k** and **1l** were predominantly olefinated at the *a*-position (**13-14**). 1,2-Disubstituted arenes **1m-1n** were olefinated by the electrooxidation at the *g*-position to furnish products **15-16**. In sharp contrast, 4-substituted anisoles **1o-1r** gave the *ortho*-substituted olefinated products **17-20** as the major products. A steric effect was predominant for *para*-chlorotoluene (**1s**). Furthermore, symmetrical trisubstituted arenes **1t** and **1u** were efficiently converted, delivering the mono-olefinated products **22** and **23**, respectively. It is noteworthy that the robust electrocatalysis proved also viable for heteroarenes. Thus, thiophene (**1v**), dibenzofuran (**1w**) and furan (**1x**) were efficiently olefinated by the palladium-electrocatalysis to yield the olefinated products **24-26** in the absence of chemical oxidants, giving molecular hydrogen by HER as the sole stoichiometric byproduct.

Thereafter, we examined the versatility of the electrocatalysis with diversely decorated alkenes **2**. Hence, a range of alkenes **2** was compatible with the versatile electrochemical conditions, providing alkenylated products **27-44**. The less congested *b*-isomer was primarily formed when *o*-xylene (**1a**) was treated with alkenylic sulphone **2b** or phosphonate **2c**. Interestingly, a considerable change in selectivity was observed when the *N,O*-ligand **L3** was employed. Thus, alkenes **2d-2g** provided the desired olefinated arenes **29-32** with a improved *b* / *a*-ratio. Likewise, a set of acrylates **2b-2e** gave high levels of *ortho*-selectivities to afford the products **33-36**. Similarly, *a,b*-unsaturated olefin **2h-2j** mirrored this position-selectivity,

providing *ortho*-olefinated products **37-39** as the major isomers. Alkenes containing a free carboxylic acid (**2g**) and 1,1-substituted double bond (**2k**) were also identified as amenable substrates (**40-41**). Furthermore, the mild nature of the palladium-electrocatalysis manifold allowed for the use of fluorinated alkene **2l**, bio-relevant cholesterol **2m**, and *NH*-free amino acid **2n**, thereby furnishing the mono-alkenylated products **42-44**.

To understand the origin of the high position-selectivity with anisoles, we conducted in depth mechanistic studies (**Fig. 3**). Here, we observed a significant improvement in position-selectivities under the electrochemical conditions as compared to reactions with commonly used chemical oxidants (**Fig. 3a**). Exploring different electrode materials revealed a remarkable dependence of the position-selectivity on the choice of the material, thereby altering the *ortho/para*-selectivity from 2:1 to remarkable 17:1 (**Fig. 3b**). Careful time-resolved analysis revealed key insights (**Fig. 3c**). The ratio of the *ortho/meta/para* selectivity remained constant for the first 12 hours of the electrooxidation, which was followed by a considerable alternation in favor of the *ortho*-functionalized product thereafter. This selectivity change was rationalized by a second chemo-selective electrooxidation event of the alkene only in the *para*-olefinated product, occurring selectively after the consumption of alkene **2a** (**Supplementary Table S11**). To substantiate this hypothesis the independently prepared *para*-olefinated product **33** was subjected to the electrochemical conditions, resulting in the formation of diacetate **46** upon acetoxylation workup (**Fig. 3d**). Control experiments clearly highlighted the essential role of the electricity for the chemo-selective two-fold electrooxidation.

The versatility of the two-fold electrooxidation was explored with a variety of electron-rich arenes in the palladaelectro-catalysis (**Fig. 3e**). Thereby, *ortho*-functionalized products **45-47** were obtained with high position-selectivity. Noteworthily, the electrocatalysis proceeded with selectivities that are complementary to the ones observed with pyridine-based ligands, which gave *para*-olefinated products as the major isomers.[27,31] Similarly, (benzyloxy)benzene derivatives and propoxybenzene gave the *ortho*-selectivily alkenylated products **48-50**. The nature of the C–H activation and its position-selectivity was studied by computing its energy profile at the PBE0-D4/def2-TZVP+SMD(AcOH)//PBE0-D3BJ/def2-SVP level of theory. The C–H activation was facile, and the formation of the *ortho*-product was preferred (**Fig. 3f**). Non-covalent interactions in the TS(1-2)^{ortho} revealed weak stabilization interactions between the anisole's ether motif and the *S,O*-ligand arene group, contributing to the preferential *ortho*-alkenylation (**Fig. 3g**).

Finally, the remarkable power of the DG-free electrocatalysis was exploited for the late-stage functionalization (LSF) of biorelevant drug molecules (**Fig. 4**).[19-21,48] The electro-C–H olefination of fenofibrate proceeded efficiently to afford the product **53**. The pain relieving drug tolmetin was selectively functionalized at the pyrrole ring to yield the mono-olefinated product **54** in 90% yield. Rivaroxaban, which prevents deep venous thrombosis, was alkenylated by the palladium-electrocatalysis to afford **55**. Bezafibrate, a commonly used lipid-lowering agent, was selectively converted to product **56**. At the same time, gemfibrozil, a drug used to reduce cholesterol blood level, was effectively converted into the corresponding alkenylated products **57**. Moreover, apremilast, a medication for the treatment of psoriasis

and psoriatic arthritis, was transformed into two separable products **58**. Indomethacin, a naonsteroidal *anti*-inflammatory drug, was position-electively olefinated to afford **59** in 66% yield. Under the chemical oxidant-free electrocatalysis, naproxen afforded olefines **60**. Estrone and its ester derivative of estrone were efficiently alkenylated at the *ortho*-position to deliver **61** and **62**, respectively, and ibuprofen was functionalized (**63**). Likewise, etodolac and ciprofibrate derivatives were chemo- and position-selectively converted in to the alkenes **64** and **65**, respectively. It is noteworthy that the robust electrocatalysis enabled the LSF of complex drug molecules by overruling the presence of various strongly coordinating directing groups, ranging from ketone and amide to ester.

We have devised a robust and versatile electrocatalytic alkenylation devoid of chemical oxidants and in the absence of directing groups. The electrochemical olefination was realized by the synergistic cooperation of electricity, a palladium catalyst and the proper electrode material. A broad variety of alkenes and arenes was amenable in the electrooxidative catalysis. A two-fold electrochemical oxidation was identified, leading to outstanding levels of selectivity in anisole functionalization. Mechanistic studies highlighted the key effect of the electrode materials towards high selectivity control. The transformative nature of the electrocatalysis strategy was reflected by late-stage diversifications of bioactive drug molecules without the installation and removal of directing groups. Overall, the electrocatalysis gives molecular hydrogen as the only stoichiometric byproduct by the hydrogen evaluation reaction (HER).

Methods

General Procedure: Non-directed electrocatalyzed olefinations. The electrocatalysis was carried out in a divided cell, equipped with a GF anode and a Pt cathode (10 mm × 15 mm × 0.25 mm). Arenes (5.0 – 20.0 equiv.), acrylates (0.20 mmol, 1.0 equiv.), $Pd(OAc)_2$ (4.5 mg, 10 mol %), ligand (20 mol %), 1,4-benzoquinone (4.3 mg, 20 mol %) and NaOAc (66 mg, 0.80 mmol) were placed in the anodic chamber and dissolved in AcOH (2.6 mL) and HFIP (1.3 mL); 1,4-benzoquinone (4.3 mg, 20 mol %) and NaOAc (66 mg, 0.80 mmol.) were placed in the cathodic chamber and dissolved in AcOH (2.6 mL) and HFIP (1.3 mL). Galvanostatic electrocatalysis was performed at 60 °C with a current of 1.0 mA and a stirring rate of 500 rpm maintained for 20 h. At ambient temperature, the resulting mixture was diluted with EtOAc (8.0 mL). The GF anode was washed with EtOAc (3 × 10 mL) in an ultrasonic bath. The combined organic phases were loaded on a column and washed with EtOAc (50 mL). The solvents were removed *in vacuo*. Then, NMR was determined by adding CH_2Br_2 (14.0 µL, 0.20 mmol, 1.0 equiv.) as the standard. The crude mixture was purified by flash column chromatography on silica gel to yield the products.

Data availability

The authors declare that the data supporting the findings of this study are available within the paper and its Supplementary Information files. Source data is provided with this paper. All other requests for materials and information should be addressed to the corresponding authors.

References

1 Fu, N., Sauer, G. S., Saha, A., Loo, A. & Lin, S. Metal-catalyzed electrochemical diazidation of alkenes. *Science* **357**, 575-579, (2017).

2 B. Zhang *et al.*, Ni-Electrocatalytic C(sp3)–C(sp3) Doubly Decarboxylative Coupling. *Nature*, (2022): 10.1038/s41586-022-04691-4.

3 Xiong, P. & Xu, H.-C. Chemistry with Electrochemically Generated N-Centered Radicals. *Acc. Chem. Res.* **52**, 3339-3350, (2019).

4 Yan, M., Kawamata, Y. & Baran, P. S. Synthetic Organic Electrochemical Methods Since 2000: On the Verge of a Renaissance. *Chem. Rev.* **117**, 13230-13319, (2017).

5 X. Dong, J. L. Roeckl, S. R. Waldvogel, B. Morandi, Merging shuttle reactions and paired electrolysis for reversible vicinal dihalogenations. *Science* **371**, 507-514 (2021).

6 T. Shen, T. H. Lambert, Electrophotocatalytic diamination of vicinal C–H bonds. *Science* **371**, 620-626 (2021).

7 Novaes, L. F. T., Liu, J., Shen, Y., Lu, L., Meinhardt, J. M. & Lin, S. Electrocatalysis as an enabling technology for organic synthesis. *Chem. Soc. Rev.* **50**, 7941-8002, (2021).

8 Meyer, T. H., Choi, I., Tian, C. & Ackermann, L. Powering the Future: How Can Electrochemistry Make a Difference in Organic Synthesis? *Chem* **6**, 2484-2496, (2020).

9 Jiao, K.-J., Xing, Y.-K., Yang, Q.-L., Qiu, H. & Mei, T.-S. Site-Selective C–H Functionalization *via* Synergistic Use of Electrochemistry and Transition Metal Catalysis. *Acc. Chem. Res.* **53**, 300-310, (2020).

10 Ackermann, L. Metalla-electrocatalyzed C–H Activation by Earth-Abundant 3d Metals and Beyond. *Acc. Chem. Res.* **53**, 84-104, (2020).

11 Ma, C., Fang, P. & Mei, T.-S. Recent Advances in C–H Functionalization Using Electrochemical Transition Metal Catalysis. *ACS Catal.* **8**, 7179-7189, (2018).

12 Kakiuchi, F. *et al.* Palladium-Catalyzed Aromatic C–H Halogenation with Hydrogen Halides by Means of Electrochemical Oxidation. *J. Am. Chem. Soc.* **131**, 11310-11311, (2009).

13 Yang, Q.-L. *et al.* Palladium-Catalyzed C(sp^3)–H Oxygenation *via* Electrochemical Oxidation. *J. Am. Chem. Soc.* **139**, 3293-3298, (2017).

14 Dhawa, U. *et al.* Enantioselective Pallada-Electrocatalyzed C–H Activation by Transient Directing Groups: Expedient Access to Helicenes. *Angew. Chem. Int. Ed.* **59**, 13451-13457, (2020).

15 Amatore, C., Cammoun, C. & Jutand, A. Electrochemical Recycling of Benzoquinone in the Pd/Benzoquinone-Catalyzed Heck-Type Reactions from Arenes. *Adv. Synth. Catal.* **349**, 292-296, (2007).

16 Sambiagio, C. *et al.* A comprehensive overview of directing groups applied in metal-catalysed C–H functionalisation chemistry. *Chem. Soc. Rev.* **47**, 6603-6743, (2018).

17 Rogge, T. *et al.* C–H activation. *Nat. Rev. Methods Primers* **1**, 43, (2021).

18 He, J., Wasa, M., Chan, K. S. L., Shao, Q. & Yu, J.-Q. Palladium-Catalyzed Transformations of Alkyl C–H Bonds. *Chem. Rev.* **117**, 8754-8786, (2017).

19 Zhang, L. & Ritter, T. A Perspective on Late-Stage Aromatic C–H Bond Functionalization. *J. Am. Chem. Soc.* **144**, 2399-2414, (2022).

20 J. Wencel-Delord, F. Glorius, C–H bond activation enables the rapid construction and late-stage diversification of functional molecules. *Nat. Chem.* **5**, 369-375 (2013).

21 Cernak, T., Dykstra, K. D., Tyagarajan, S., Vachal, P. & Krska, S. W. The medicinal chemist's toolbox for late stage functionalization of drug-like molecules. *Chem. Soc. Rev.* **45**, 546-576, (2016).

22 Meng, G. *et al.* Achieving Site-Selectivity for C–H Activation Processes Based on Distance and Geometry: A Carpenter's Approach. *J. Am. Chem. Soc.* **142**, 10571, (2020).

23 D. A. Colby, R. G. Bergman, J. A. Ellman, Rhodium-Catalyzed C–C Bond Formation via Heteroatom-Directed C–H Bond Activation. *Chem. Rev.* **110**, 624–655 (2010).

24 Lewis, J. C., Coelho, P. S. & Arnold, F. H. Enzymatic functionalization of carbon–hydrogen bonds. *Chem. Soc. Rev.* **40**, 2003-2021, (2011).

25 Wedi, P. & van Gemmeren, M. Arene-Limited Nondirected C–H Activation of Arenes. *Angew. Chem. Int. Ed.* **57**, 13016-13027, (2018).

26 Jia, C., Kitamura, T. & Fujiwara, Y. Catalytic Functionalization of Arenes and Alkanes *via* C–H Bond Activation. *Acc. Chem. Res.* **34**, 633-639, (2001).

27 Wang, P. *et al.* Ligand-accelerated non-directed C–H functionalization of arenes. *Nature* **551**, 489-493, (2017).

28 Zhang, Y.-H., Shi, B.-F. & Yu, J.-Q. Pd(II)-Catalyzed Olefination of Electron-Deficient Arenes Using 2,6-Dialkylpyridine Ligands. *J. Am. Chem. Soc.* **131**, 5072-5074, (2009).

29 Cook, A. K. & Sanford, M. S. Mechanism of the Palladium-Catalyzed Arene C–H Acetoxylation: A Comparison of Catalysts and Ligand Effects. *J. Am. Chem. Soc.* **137**, 3109-3118, (2015).

30 Cook, A. K., Emmert, M. H. & Sanford, M. S. Steric Control of Site Selectivity in the Pd-Catalyzed C–H Acetoxylation of Simple Arenes. *Org. Lett.* **15**, 5428-5431, (2013).

31 Kubota, A., Emmert, M. H. & Sanford, M. S. Pyridine Ligands as Promoters in $Pd^{II/0}$-Catalyzed C–H Olefination Reactions. *Org. Lett.* **14**, 1760-1763, (2012).

32 Emmert, M. H., Cook, A. K., Xie, Y. J. & Sanford, M. S. Remarkably High Reactivity of $Pd(OAc)_2$/Pyridine Catalysts: Nondirected C–H Oxygenation of Arenes. *Angew. Chem. Int. Ed.* **50**, 9409-9412, (2011).

33 Izawa, Y. & Stahl, S. S. Aerobic Oxidative Coupling of *o*-Xylene: Discovery of 2-Fluoropyridine as a Ligand to Support Selective Pd-Catalyzed C–H Functionalization. *Adv. Synth. Catal.* **352**, 3223-3229, (2010).

34 Wedi, P., Farizyan, M., Bergander, K., Mück-Lichtenfeld, C. & van Gemmeren, M. Mechanism of the Arene-Limited Nondirected C–H Activation of Arenes with Palladium. *Angew. Chem. Int. Ed.* **60**, 15641-15649, (2021).

35 Mondal, A. & van Gemmeren, M. Catalyst-Controlled Regiodivergent C–H Alkynylation of Thiophenes. *Angew. Chem. Int. Ed.* **60**, 742-746 (2021).

36 Farizyan, M., Mondal, A., Mal, S., Deufel, F. & van Gemmeren, M. Palladium-Catalyzed Nondirected Late-Stage C–H Deuteration of Arenes. *J. Am. Chem. Soc.* **40**, 16370–16376, (2021).

37 Chen, H., Farizyan, M., Ghiringhelli, F. & van Gemmeren, M. Sterically Controlled C–H Olefination of Heteroarenes. *Angew. Chem. Int. Ed.* **59**, 12213-12220, (2020).

38 Mondal, A., Chen, H., Flämig, L., Wedi, P. & van Gemmeren, M. Sterically Controlled Late-Stage C–H Alkynylation of Arenes. *J. Am. Chem. Soc.* **141**, 18662-18667, (2019).

39 Chen, H., Wedi, P., Meyer, T., Tavakoli, G. & van Gemmeren, M. Dual Ligand-Enabled Nondirected C–H Olefination of Arenes. *Angew. Chem. Int. Ed.* **57**, 2497-2501, (2018).

40 Sukowski, V., Jia, W.-L., van Diest, R., van Borselen, M. & Fernández-Ibáñez, M. Á. S,O-Ligand-Promoted Pd-Catalyzed C–H Olefination of Anisole Derivatives. *Eur. J. Org. Chem.* 4132-4135, (2021).

41 Naksomboon, K., Poater, J., Bickelhaupt, F. M. & Fernández-Ibáñez, M. Á. *para*-Selective C–H Olefination of Aniline Derivatives *via* Pd/S,O-Ligand Catalysis. *J. Am. Chem. Soc.* **141**, 6719-6725, (2019).

42 Jia, W.-L. *et al.* Selective C–H Olefination of Indolines (C5) and Tetrahydroquinolines (C6) by Pd/S,O-Ligand Catalysis. *Org. Lett.* **21**, 9339-9342, (2019).

43 Naksomboon, K., Valderas, C., Gómez-Martínez, M., Álvarez-Casao, Y. & Fernández-Ibáñez, M. Á. S,O-Ligand-Promoted Palladium-Catalyzed C–H Functionalization Reactions of Nondirected Arenes. *ACS*

Catal. **7**, 6342-6346, (2017).

44 Ramadoss, B., Jin, Y., Asako, S. & Ilies, L. Remote steric control for undirected *meta*-selective C–H activation of arenes. *Science* **375**, 658-663, (2022).

45 Kuninobu, Y., Ida, H., Nishi, M. & Kanai, M. A *meta*-selective C–H borylation directed by a secondary interaction between ligand and substrate. *Nat. Chem.* **7**, 712-717, (2015).

46 Gorsline, B. J., Wang, L., Ren, P. & Carrow, B. P. C–H Alkenylation of Heteroarenes: Mechanism, Rate, and Selectivity Changes Enabled by Thioether Ligands. *J. Am. Chem. Soc.* **139**, 9605-9614, (2017).

47 Bruns, D. L., Musaev, D. G. & Stahl, S. S. Can Donor Ligands Make $Pd(OAc)_2$ a Stronger Oxidant? Access to Elusive Palladium(II) Reduction Potentials and Effects of Ancillary Ligands *via* Palladium(II)/Hydroquinone Redox Equilibria. *J. Am. Chem. Soc.* **142**, 19678-19688, (2020).

48 Zhao, D., Xu, P. & Ritter, T. Palladium-Catalyzed Late-Stage Direct Arene Cyanation. *Chem* **5**, 97-107, (2019).

Declarations

Acknowledgements

Generous support by the ERC Advanced Grant no.101021358, the DFG (Gottfried-Wilhelm-Leibniz award and SPP 1807), the European Union H2020 research and innovation program under the Marie S. Curie Grant Agreement No 860762 (CHAIR), the CSC (scholarship to Z.L. and B.Y.), the DAAD (fellowship to U.D.) and the Ministry of Science and Technology, Taiwan (scholarship 110-2917-I-003-002 to Y.-C.L.) is gratefully acknowledged.

Author contributions

Conceptualization, L.A.; Methodology, U.D., Z.L., L.A.; Experiment, Z.L., Y.-C.L. and U.D.; DFT, B.Y.; Writing, contributed by all authors; Funding Acquisition, L.A.; Resources, L.A.; Supervision, L.A.

Conflict of interest

The authors declare no conflict of interest.

Figures

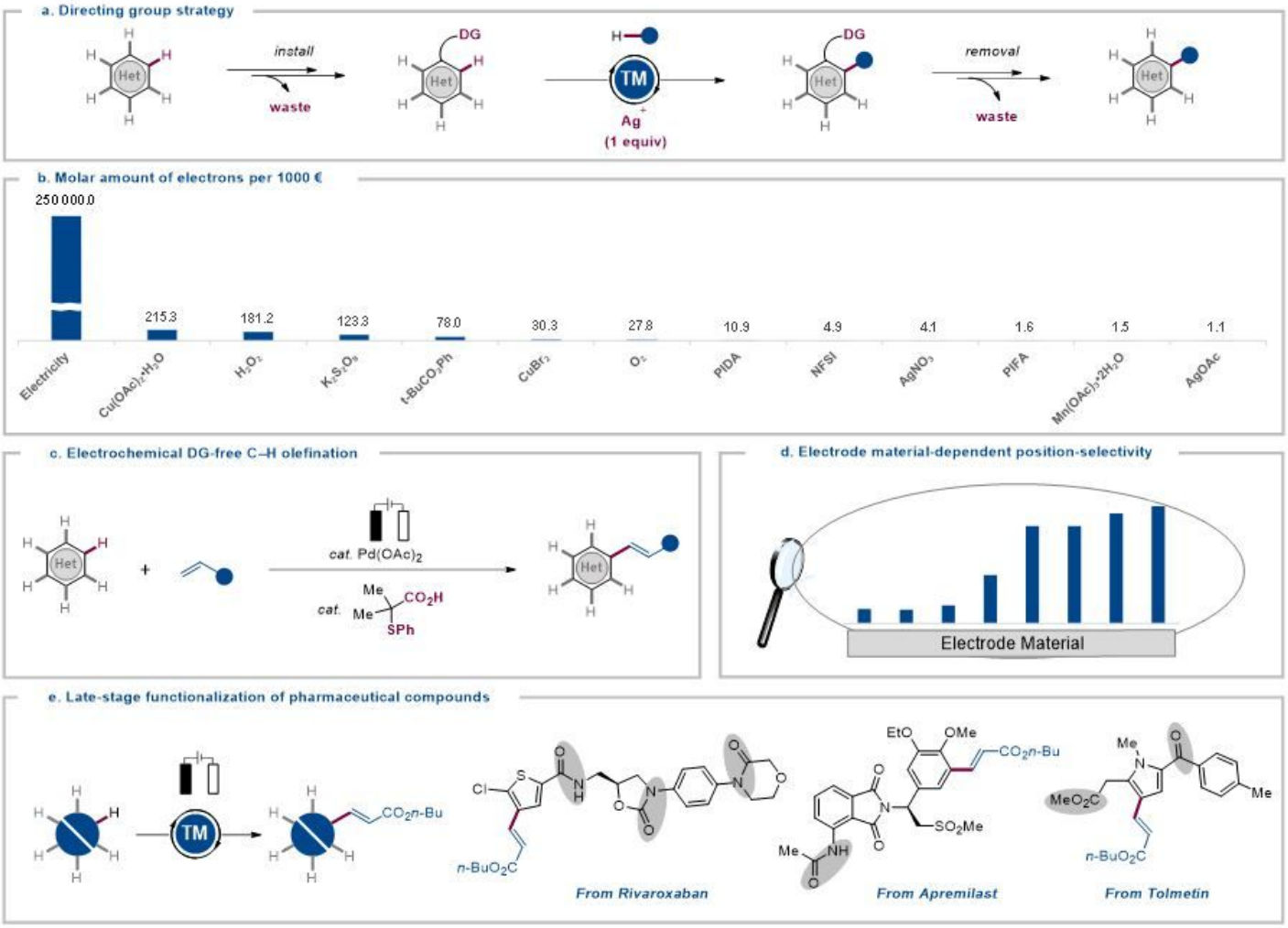

Figure 1

Directing group (DG)-free electrochemical C–H activation. a, Directing group (DG)-assisted oxidative C–H activation by installation and removal of DG. b, Molar amount of electrons per 1000 euro from electricity and chemical oxidants. PIFA = (bis(trifluoroacetoxy)iodine)benzene. NFSI = *N*-Fluorobenzenesulfonimide. PIDA = (Diacetoxyiodo)benzene. c, Electrochemical DG-free C–H olefination. d, Effects of the electrode material onto position-selectivity. e, Late-stage functionalization of pharmaceutical molecules. (potential DG was highlighted in grey).

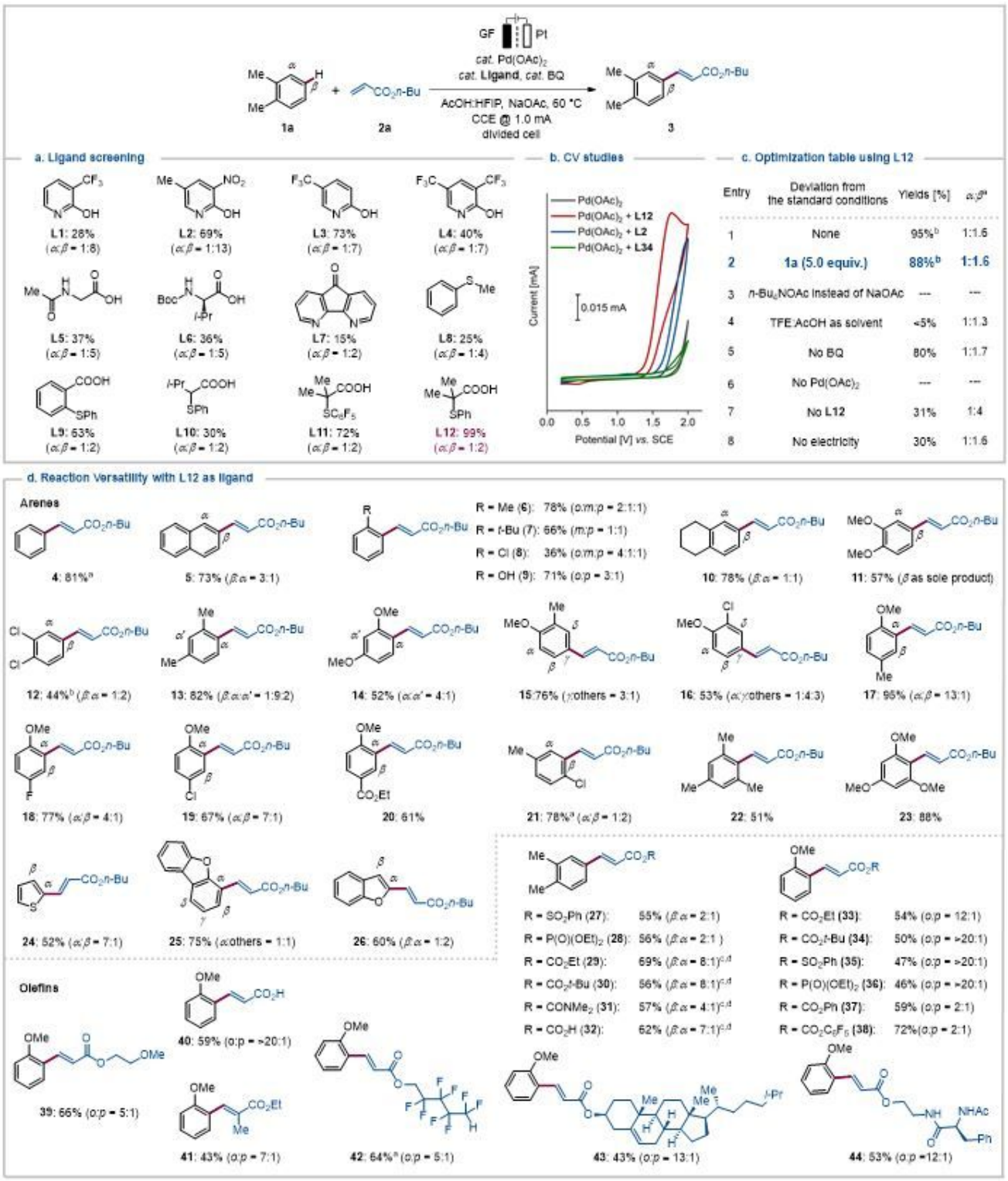

Figure 2

Optimization studies and Substrate Scope. See supplementary information for reaction details. a, Ligand optimization for the DG-free electrochemical alkenylation of arene 1a. b, Cyclic voltammograms in AcOH:HFIP (2:1) with n-Bu_4NPF_6 (0.1 M) at 100 mV/s, a) $Pd(OAc)_2$ (5.0 mM), ligand (10 mM). c, Optimization of DG-free palladium-electrocatalysis. [a] Determined by crude ^{1}H-NMR with CH_2Br_2 as the

internal standard. [b] Isolated yield. d, DG-Free Palladium-Electrocatalyzed C–H Activation. [a] 80 °C. [b] 100 °C. [c] 1 (20 equiv.). [d] L3 (20 mol %) was used instead of L12. BQ = 1,4-Benzoquinone. TFE = 2,2,2-Trifluoroethanol.

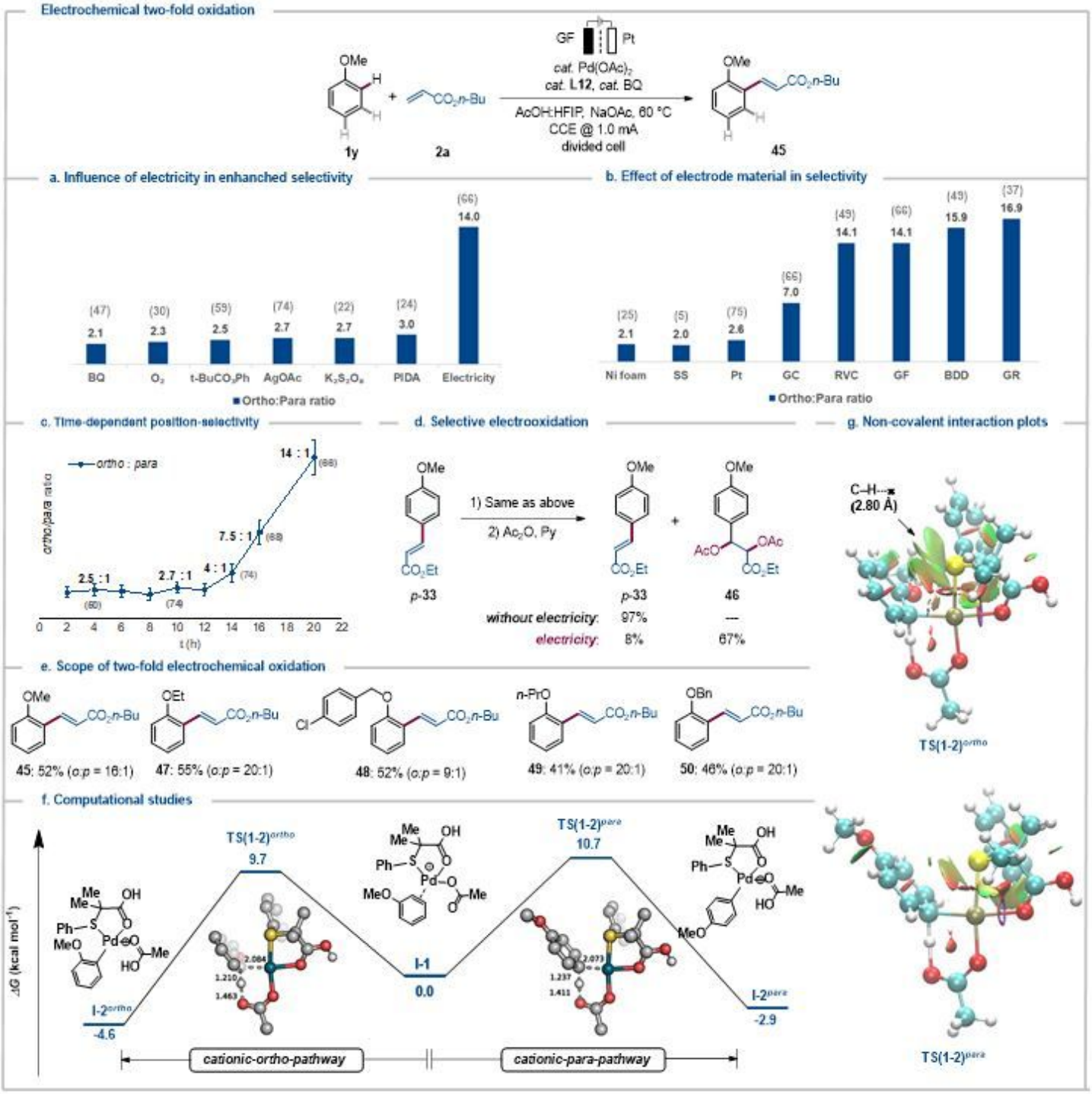

Figure 3

Mechanistic study for electrochemical two-fold oxidation. **a**, Chemical oxidants *vs* Electricity. **b**, Variation of anode materials. RVC = Reticulated vitreous carbon. GF = Graphite felt. BDD = Boron doped diamond. GR = Graphite rod. **c**, *ortho/para*-selectivity profile. Combined yields of *ortho/para*-isomers were given in

the parenthesis. **d**, Selective oxidation of *para*-olefinated product. **e**, Scope of two-fold oxidation. **f**, Computed relative Gibbs free energy profile ($\Delta G_{333.15}$) in kcal mol^{-1} for cationic C–H activation pathways at the PBE0-D4/def2-TZVP+SMD(AcOH)//PBE0-D3BJ/def2-SVP level of theory. Non-participating hydrogen atoms in the transition state structures were omitted, with bond lengths given in Å. **g.** Non-covalent interaction plots for the TS(1-2)^{ortho} and TS(1-2)^{para}.

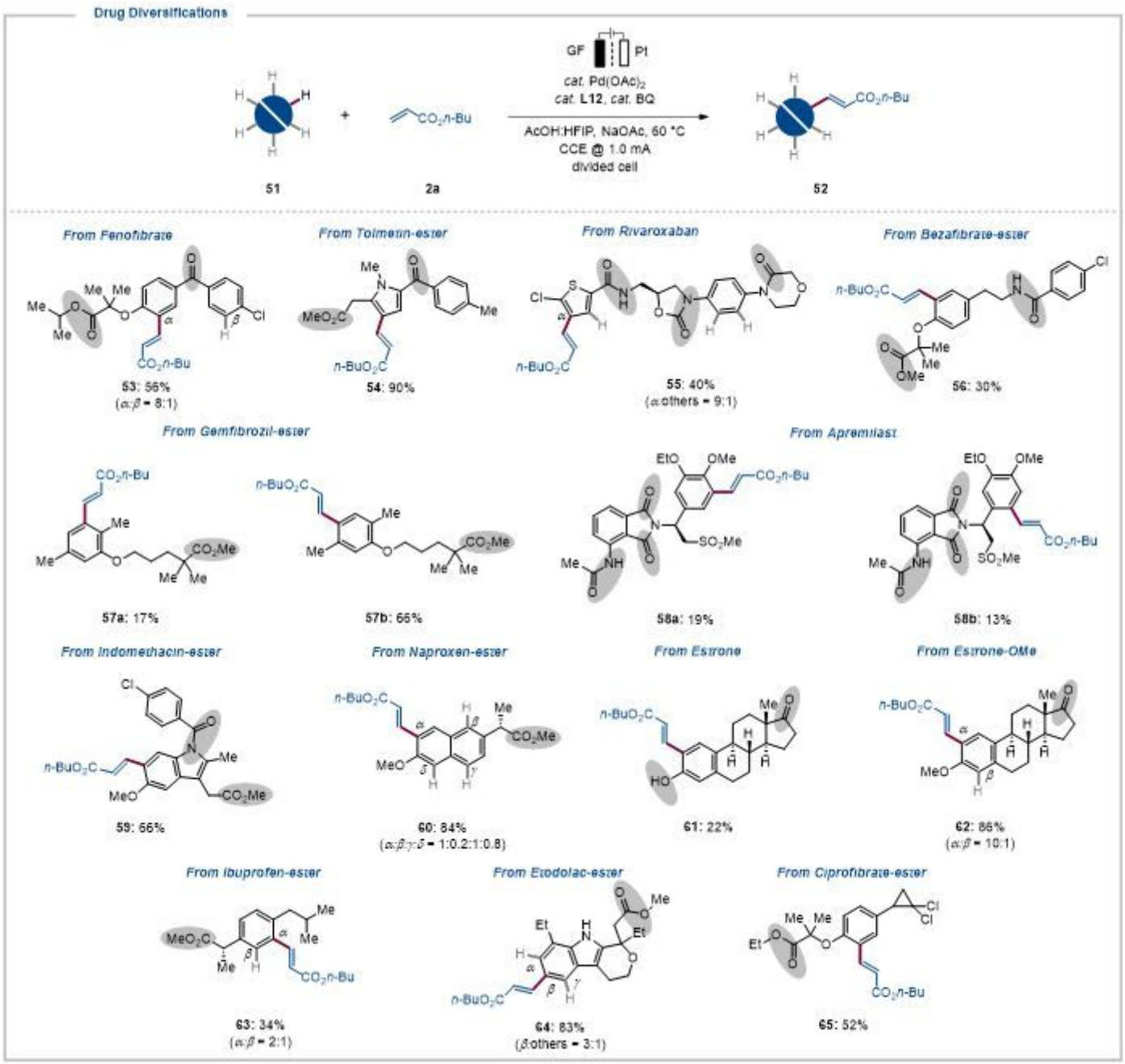

Figure 4

Late-Stage Functionalization of Drug Molecules. See supporting information for details. Potential coordinating directing groups are highlighted in grey.

Supplementary Files

This is a list of supplementary files associated with this preprint. Click to download.

- SIelectrochemicalPdnondirectedcholefination.pdf